β-Cell DNA Damage Response Promotes Islet Inflammation in Type 1 Diabetes

Elad Horwitz,[1] Lars Krogvold,[2] Sophia Zhitomirsky,[1] Avital Swisa,[1] Maya Fischman,[1] Tsuria Lax,[1] Tehila Dahan,[1] Noa Hurvitz,[1] Noa Weinberg-Corem,[1] Agnes Klochendler,[1] Alvin C. Powers,[3,4] Marcela Brissova,[3] Anne Jörns,[5] Sigurd Lenzen,[5,6] Benjamin Glaser,[7] Knut Dahl-Jørgensen,[2] and Yuval Dor[1]

Diabetes 2018;67:2305–2318 | https://doi.org/10.2337/db17-1006

Type 1 diabetes (T1D) is an autoimmune disease where pancreatic β-cells are destroyed by islet-infiltrating T cells. Although a role for β-cell defects has been suspected, β-cell abnormalities are difficult to demonstrate. We show a β-cell DNA damage response (DDR), presented by activation of the 53BP1 protein and accumulation of p53, in biopsy and autopsy material from patients with recently diagnosed T1D as well as a rat model of human T1D. The β-cell DDR is more frequent in islets infiltrated by CD45$^+$ immune cells, suggesting a link to islet inflammation. The β-cell toxin streptozotocin (STZ) elicits DDR in islets, both in vivo and ex vivo, and causes elevation of the proinflammatory molecules IL-1β and Cxcl10. β-Cell–specific inactivation of the master DNA repair gene ataxia telangiectasia mutated (ATM) in STZ-treated mice decreases the expression of proinflammatory cytokines in islets and attenuates the development of hyperglycemia. Together, these data suggest that β-cell DDR is an early event in T1D, possibly contributing to autoimmunity.

Type 1 diabetes (T1D) is a metabolic disorder that develops after an autoimmune attack on pancreatic β-cells. Emerging evidence has suggested that β-cell defects may play a causal or enabling role in the development of T1D. Analysis of islets from patients with recently diagnosed T1D has revealed that many islets retain an intact structure with minimal evidence of immune cell infiltration and preservation of as much as 36% of β-cell mass at disease onset (1). β-Cell dysfunction in such patients, therefore, may result from a functional defect rather than from only immune destruction (2,3). However, scarce evidence currently is available for early β-cell defects in T1D partly because of limited access to material from recently diagnosed patients.

We have previously reported that metabolic stress, driven by hyperglycolysis, activates a DNA damage response (DDR) in β-cells in mouse models as well as in patients with type 2 diabetes (4). Although the findings suggested DNA damage as a novel player in β-cell dysfunction, the functional impact of this phenomenon remains unclear. Genetic disruption of some DDR components in mice does affect β-cell biology (5). For example, mutation in DNA ligase IV leads to spontaneous β-cell apoptosis and insulin-dependent hyperglycemia (6). On the other hand, mice deficient for the Ku70 DNA damage sensor show increased β-cell proliferation and are hypoglycemic (7). In addition, another study suggested that genetic polymorphisms in genes participating in DNA double-strand break repair (XRCC4 and DNA ligase IV) may predispose to β-cell dysfunction in T1D (8). Given this body of evidence and the established, bidirectional links

[1]Department of Developmental Biology and Cancer Research, The Hebrew University, Jerusalem, Israel
[2]Paediatric Department, Oslo University Hospital HF, Faculty of Medicine, University of Oslo, Oslo, Norway
[3]Division of Diabetes, Endocrinology, and Metabolism, Department of Medicine, Vanderbilt University Medical Center, and Department of Molecular Physiology and Biophysics, Vanderbilt University School of Medicine, Nashville, TN
[4]Veterans Affairs Tennessee Valley Healthcare System, Nashville, TN
[5]Institute of Clinical Biochemistry, Hannover Medical School, Hannover, Germany
[6]Institute of Experimental Diabetes Research and Institute of Clinical Biochemistry, Hannover Medical School, Hannover, Germany
[7]Endocrinology and Metabolism Service, Hadassah-Hebrew University Medical Center, Jerusalem, Israel

Corresponding author: Yuval Dor, yuvald@ekmd.huji.ac.il, or Knut Dahl-Jørgensen, knut.dahl-jorgensen@medisin.uio.no.

Received 23 August 2017 and accepted 18 August 2018.

This article contains Supplementary Data online at http://diabetes.diabetesjournals.org/lookup/suppl/doi:10.2337/db17-1006/-/DC1.

K.D.-J. and Y.D. are shared senior authors.

K.D.-J. is principal investigator of the Diabetes Virus Detection (DiViD) study.

between DNA damage and immune system activation in cancer (9), we assessed the β-cell DDR in recent-onset human and rodent T1D and the potential contribution of DDR to islet inflammation.

RESEARCH DESIGN AND METHODS

Immunostaining

Sections from formalin-fixed paraffin-embedded donor-derived pancreata were obtained from the Network for Pancreatic Organ Donors With Diabetes (nPOD) repository, the Diabetes Virus Detection (DiViD) study, and the tissue bank of A.C.P. at Vanderbilt University (including age-matched control subjects without diabetes). Full details on all donors are listed in Supplementary Table 1. Paraffin sections were rehydrated, and antigen retrieval was performed in a decloaking chamber (Biocare Medical) in 50 mmol/L citrate buffer (pH 6). The following primary antibodies were used: guinea pig anti-insulin (1:400; DAKO), mouse antiglucagon (1:200; Abcam), rabbit anti-53BP1 (1:200; Bethyl), mouse anti-γ−H2AX Ser139 (1:3,000; Millipore), mouse anti-CD45 (1:100; DAKO), rabbit antiphosphorylated (phospho)-Kap1 (1:100; Bethyl), rabbit anti-p53 (1:400; Novocastra), rat anti-CD3 (1:300; Millipore), and rabbit anti–human growth hormone (hGH) (1:200; Abcam). Fluorophore-conjugated secondary antibodies used were donkey anti–guinea pig Alexa Fluor 488, donkey anti-rabbit Cy3/Cy5, and donkey anti-mouse Alexa Fluor 488/Cy3 (The Jackson Laboratory). DAPI (Invitrogen) was used as a nuclei marker. Horseradish peroxidase–conjugated secondary antibody was donkey anti-rabbit (Histofine; Nichirei Biosciences). Diaminobenzidine (Lab Vision) was used as chromogen. Fluorescent images were taken with a Nikon C1 confocal microscope at 400× magnification. Bright-field images were taken with an Olympus BX53 at 400× magnification. Image quantification was performed using the ImageJ software.

Statistics

Data were analyzed using a paired two-tail Student *t* test (for two-group comparisons), two-way ANOVA for repeated measures, and log-rank test for Kaplan-Meier analyses. Data were processed using Microsoft Excel 2010. Graphs were generated using GraphPad Prism 5.0 and Excel. Error bars represent 1 SEM.

Animal Studies

Animal experiments were approved by the institutional animal care and use committee of The Hebrew University. The Hebrew University is an AAALAC International–accredited institute. NOD mice were purchased from Harlan Laboratories. Floxed *Atm* mice (10) and Rip-Cre mice (11) were purchased from The Jackson Laboratory and housed in The Hebrew University specific-pathogen-free facility. The genetic background was mixed ICR and SV129. For the ex vivo and streptozotocin (STZ)-caffeine experiments, we used 2-month-old male ICR mice purchased from Envigo. STZ (Sigma) was dissolved in citrate buffer (pH 4.5) immediately before injections and was administrated intraperitoneally for 5 consecutive days to mice that were starved for 4–6 h before injection. A variety of STZ doses were tested; selected doses were the highest that did not result in hyperglycemic mice during the injection days (30 mg/kg for females, 20 mg/kg for males). Acute single-dose STZ was administered at 200 mg/kg. Caffeine (Sigma) was dissolved in saline (50 mg/kg) and administered intraperitoneally along with STZ (20 mg/kg). Irradiation of mice in a confined perspex cage was performed in a DBX 6× machine (Varian) with an Eclipse 13.0 Treatment Planning System. Serum insulin was measured using an ELISA kit (Crystal Chem). DDR in LEW.1AR1-iddm rats (12,13) was assessed using archived histological material.

Mouse Islets

Islet isolation was performed as previously described (14). Briefly, mice were euthanized and the bile duct clamped at the duodenal entry. Collagenase P (0.4 mg/mL; Roche) was perfused into the bile duct. Pancreata were then removed and incubated for 15 min at 37°C. Samples were washed with RPMI medium (Gibco) and then loaded on Ficoll (1.119 g/mL density), and a layer of Ficoll (1.079 g/mL density) was added above. Samples were centrifuged at 1,250*g* for 20 min. Islets floating in the upper phase were pipetted from the gradient, washed in RPMI medium, and manually picked under a binocular. For ex vivo experiments, islets were kept in RPMI media. Islets were treated with STZ (5 mmol/L; Sigma), neocarzinostatin (0.5 μg/mL; Sigma), and the ATM inhibitor KU55933 (10 μmol/L; Biovision) or mouse tumor necrosis factor-α (TNF-α) (aa 80-235, 1,000 IU/mL; R&D Systems).

DNA and RNA Analyses

DNA was produced with a QIAGEN DNeasy Kit. DNA PCR reactions were performed with GoTaq Green Master Mix on a PTC-200 thermal cycler (MJ Research). DNA primer sequences were as follows: ATM57F-5′-GCTAAGCCTG-ACCACCTGAG-3′, ATM58F-5′-CTTTAATGTGCCTCCCT-TCG-3′, ATM58R-5′-GAAGGATCTTCCCCTGTTCA-3′, Cre F-5′-TGCCACGACCAAGTGACAGC-3′, Cre R-5′-CCAGGTTAC-GGATATAGTTCATG-3′. PCR products were electrophoresed on 2% agarose gels (Invitrogen) and imaged with ethidium bromide (AMRESCO) and were documented using a UVP BioDoc-It Benchtop ultraviolet transilluminator.

RNA was isolated with TRIzol (Invitrogen). Reverse transcription was performed with a qScript kit (Quanta). Quantitative PCR (qPCR) was performed on a CFX384 thermal cycler with PerfeCTa SYBR Green SuperMix (Quanta). Primer sequences for qPCR are listed in Supplementary Table 2.

RESULTS

DDR in β-Cells Shortly After T1D Diagnosis

To explore changes in β-cells during the development of human T1D, we used histological specimens from the

pancreata of donors with different durations of T1D. We assessed the DDR in samples from T1D-prone, autoantibody-positive (AAB+) individuals; patients with recently diagnosed T1D (1–9 weeks from diagnosis, median 4 weeks); patients with established T1D (only samples in which insulin-positive cells could still be observed, 0.6–32.5 years from diagnosis); and healthy control donors. The recently diagnosed T1D group included material from cadaveric donors obtained from nPOD (n = 3, diagnosed ~1 week before death) (15), and, importantly, samples taken from pancreatic tail resections of six live patients included in the DiViD study (1,16). The latter are of exceptional histological quality because the time from tissue sampling to fixation was minimal. However, we were able to detect significant numbers of β-cells only in four of these samples. The clinical data of all donors are summarized in Table 1 and in Supplementary Table 1.

We first examined the staining pattern of 53BP1, an established marker of the DDR that is recruited to sites of double-strand breaks in the DNA (17). We determined the staining pattern of 53BP1 in β-cells of mice exposed to high-dose, sublethal γ-irradiation (5 Gy) 8 h before sacrifice. As shown in Fig. 1*A* and Supplementary Fig. 1*A*, β-cells of irradiated mice showed a typical accumulation of 53BP1 in a single, large nuclear focus. This pattern is reminiscent of the large nuclear foci previously reported to mark unrepairable DNA damage (18). These findings support the idea that the 53BP1 foci mark the cellular DDR, and their presence indicates the presence of DNA double-stand breaks.

Although most β-cells in human samples showed a diffuse pattern of nuclear 53BP1, a minority showed a single large nuclear focus of 53BP1 like those observed in mice after γ-irradiation (Fig. 1*A*). We quantified the effect by scoring the fraction of insulin-stained cells that have a large 53BP1 nuclear focus (Fig. 1*B*). Compared with the healthy control group (nuclear foci in 0.658 ± 0.15% of β-cells), we found a significant increase of the 53BP1-positive fraction in both the AAB+ group (1.52 ± 0.15% of β-cells; $P < 0.01$) and the established T1D group (1.536 ± 0.28%; $P < 0.05$). Of note, samples from patients with recently diagnosed T1D showed the most significant elevation in the proportion of β-cells that scored positive (2.99 ± 0.52%; $P < 0.0001$), suggesting that the β-cell DDR may peak near diagnosis. The extent of 53BP1 activation in β-cells did not correlate with age, sex, C-peptide levels, BMI, duration of disease, or number of AAB types (data not shown). Because our samples originated from various sources (different centers and from both live and cadaveric donors), we performed a comparison of samples belonging to the same clinical group. We found significant differences between nPOD samples and A.C.P. laboratory samples in the healthy control group (Supplementary Fig. 1*B*) and between nPOD and DiViD samples in the recently diagnosed T1D group (Supplementary Fig. 1*C*). The differences may result from the condition of donors before tissue fixation (live biopsy vs. cadaveric samples). However, significant differences between control subjects and patients were observed even when examining only the subset of samples originating from nPOD (Supplementary Fig. 1*D*). We conclude that intersource differences exist but do not mask the differences between control subjects and patients.

To determine the cell specificity of the DDR in T1D, we assessed the activation of 53BP1 in other pancreatic cell types. First, we examined cells of the exocrine pancreas, given evidence for the involvement of the exocrine pancreas in T1D (19,20). We observed a large variation among individuals recently diagnosed with T1D, but the difference between control subjects and recently diagnosed patients did not reach statistical significance (control subjects 1.59 ± 0.578% positive acinar cells, patients with recently diagnosed T1D 3.66 ± 1.12% labeled acinar cells; P = 0.09). The fraction of positive acinar cells in recent-onset T1D appeared to higher than in samples from established T1D (0.88 ± 0.24%; $P < 0.05$) (Supplementary Fig. 2*A*). There were no significant differences in the 53BP1 pattern among glucagon-expressing α-cells from

Table 1—Summary of donor clinical data

	Donor type			
	Control	AAB+	Recently diagnosed with T1D	Established T1D
n	12	20	7	18
β-Cells with activated 53BP1 (%)	0.547 ± 0.21	1.606 ± 0.25	3.00 ± 0.51	1.629 ± 0.49
Number of AABs	0	1.33 ± 0.19	2.333 ± 0.50	1.55 ± 0.60
Age (years)	23.7 ± 3.6	43.81 ± 5.8	24.7 ± 3.1	27.6 ± 2.7
Sex				
Male (%)	67	67	56	33
Female (%)	33	33	44	67
C-peptide (ng/mL)	7.02 ± 1.38	9.30 ± 3.42	0.23 ± 0.05	0.98 ± 0.53
HbA_{1c}	5.40 ± 0.21	6.25 ± 0.22	9.20 ± 1.02	8.80 ± 0.91
BMI from chart (kg/m^2)	24.97 ± 1.78	26.68 ± 2.31	23.00 ± 1.86	23.19 ± 1.18

Data are mean ± SD, unless stated otherwise.

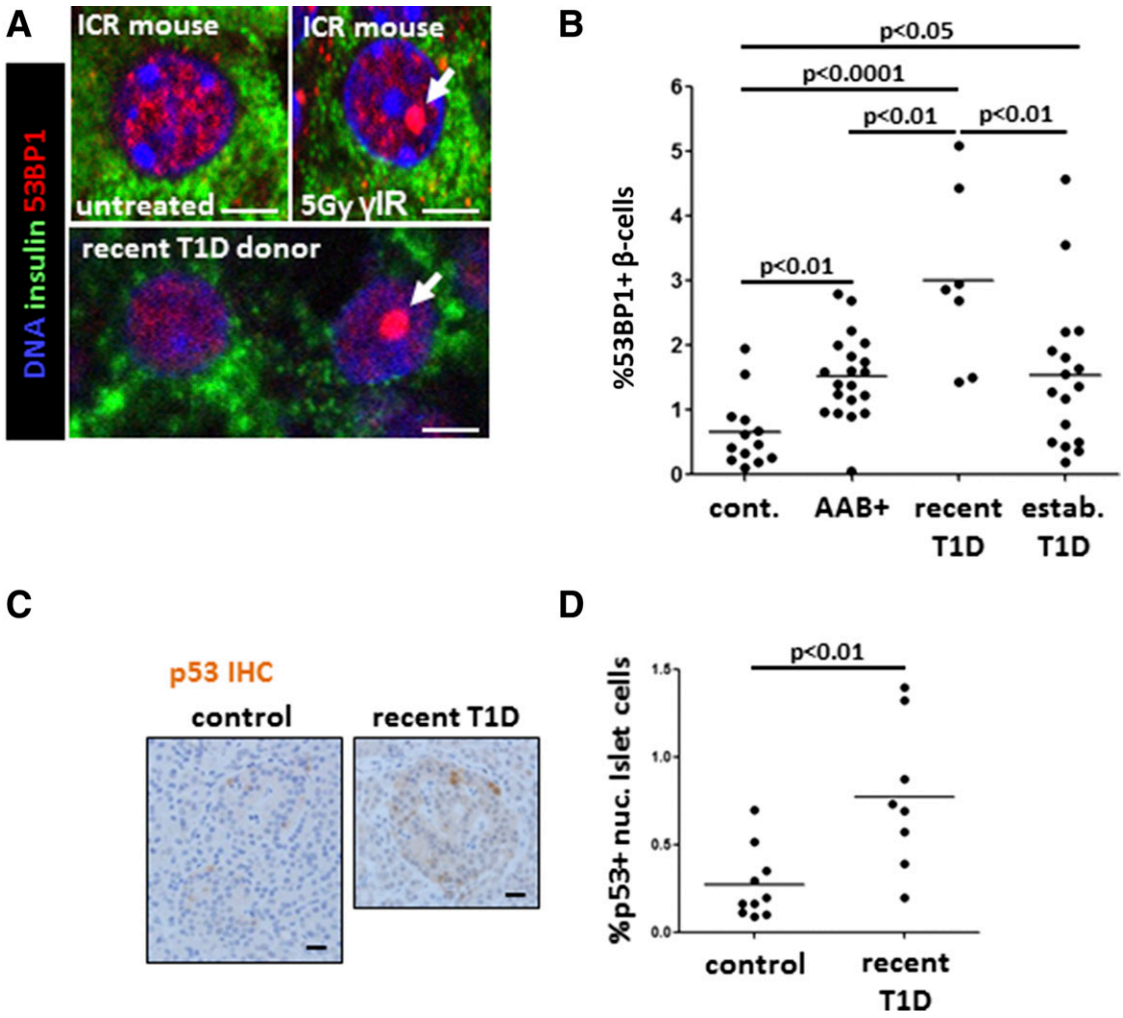

Figure 1—DDR in β-cells of patients with recently diagnosed T1D. *A*: Immunofluorescent staining of 53BP1 in β-cells in vivo. The top panel shows the pattern of nuclear 53BP1 in β-cells (stained for insulin) of wild-type mice, untreated or 8 h after sublethal γ-irradiation (γIR). Note the typical accumulation of a large, single nuclear focus of 53BP1 in irradiated mice (arrow). The bottom panel shows two adjacent β-cells from patients with recently diagnosed T1D, with the normal or DNA damage typical pattern of nuclear 53BP1 (arrow). Scale bars = 2 μm. *B*: The fraction of β-cells with activated 53BP1 in healthy donors (cont.) (n = 12), people at risk for T1D (AAB+, n = 20), patients with recently diagnosed T1D (n = 7), and patients with established T1D (n = 18). Each dot represents an individual person. *C*: Representative images from immunostaining for p53 in islets of health donors and patients recently diagnosed with T1D. Nuclear accumulation of signal signifies p53 activation. Scale bars = 20 μm. *D*: Quantification of nuclear (nuc.) p53 in islets from healthy donors (n = 10) and patients with recently diagnosed T1D (n = 7). Each dot represents an individual person. IHC, immunohistochemistry.

healthy control subjects and patients with recently diagnosed T1D (2.88 ± 0.49% and 2.42 ± 0.40, respectively) (Supplementary Fig. 2*B*). These results suggest that a heightened DDR exists in the pancreas of patients with recently diagnosed T1D and that the elevated response is largely restricted to β-cells.

Consistent with heightened DDR, we observed in recent-onset T1D a significant increase in the fraction of islet cells that stained for p53, a transcription factor that is stabilized after cellular insults, including DNA damage (control islets 0.288 ± 0.07% p53-positive cells, islets of recent-onset T1D 0.78 ± 0.17% p53-positive cells; $P < 0.01$) (Fig. 1*C* and *D*). These findings further support the idea that β-cells in the early stages of T1D have excessive DNA breaks and a subsequent cellular response. Other markers of DDR activation, including the phosphorylated forms of ATM, Kap1, and H2AX, were scarce in the human T1D samples (data not shown) potentially because of the short half-life of these phosphorylation events in β-cells after DNA damage (Supplementary Fig. 1*A* and data not shown).

The β-Cell DNA Damage Response Is Associated With Islet Inflammation

The islets of patients with recently diagnosed T1D have a heterogeneous morphology. Some islets are heavily infiltrated by immune cells (insulitis), whereas other islets from the same individual and in the same histological section appear intact, presumably captured in the midst of the pathogenic process. We took advantage of this heterogeneity to ask whether immune infiltration status is locally

correlated to β-cell DDR. Within the recently diagnosed T1D group, islets or islet remnants with a higher index of 53BP1 tended to be surrounded by larger masses of cells with small nuclei (Fig. 2*A*). Coimmunostaining of 53BP1 with the pan-leukocyte marker CD45 confirmed that infiltrating cells were leukocytes (Fig. 2*A*, inset). To quantify the link between DDR in β-cells and immune cell infiltration, we assigned to each islet an immune infiltration grade according to the pattern of the CD45 staining (no infiltration and minor, mild, moderate, and severe insulitis) (Fig. 2*B* and Supplemental Fig. 2*C*). We then quantified the extent of activated 53BP1 in β-cells of patients with recently diagnosed T1D according to this classification (with the scoring of each islet done while blinded to the score of the other parameter). The percentage of β-cells with a 53BP1 nuclear focus was higher in islets with a more severe immune infiltration (Fig. 2*C*), and the differences reached statistical significance, with as much as 10.5% of β-cells stained positive for 53BP1 in islets scored as severely infiltrated. These findings reveal a positive association between the DDR in β-cells and islet immune infiltration.

Assessing Physical Proximity Between Immune Cells and β-Cells With DDR

DNA damage and inflammation may trigger each other (21). The innate and adaptive immune systems can inflict DNA damage to target cells, including β-cells (22), typically through direct cell-cell interactions (23,24). On the other hand, DNA damage may trigger an inflammatory immune response, typically through secreted factors (22,25–27). We assessed the spatial relationship between 53BP1-activated β-cells and islet-infiltrating cells by counting the fraction of 53BP1-positive β-cells that were in direct contact with $CD45^+$ cells or separated from immune cells by at least one islet cell layer (Fig. 2*D*). Only a minority of β-cells with activated 53BP1 was in physical proximity to cells of immune origin (20.17% of 53BP1-positive cells physically adjacent to immune-infiltrating cells) (Fig. 2*E*). These findings suggest that the β-cell DDR in recent-onset T1D is unlikely a mere response to factors from immediately adjacent immune cells.

DDR Signaling in Rodent Models of T1D

To assess the generality of DDR in autoimmune diabetes, we turned to rodent models. One classic model of diabetes in mice is based on treatment with STZ, a β-cell–selective toxin that induces DNA damage through both alkylation and the generation of reactive oxygen and nitrogen species (28). We used the multiple low-dose STZ (MLDS) model where five daily sublethal injections of STZ trigger hyperglycemia within 2 weeks (29). To examine whether the MLDS model recapitulated the β-cell DDR observed in patients with recently diagnosed T1D, we quantified 53BP1 in islets of wild-type mice injected with a low dose of STZ. Within 8 h of STZ injection, there was a marked increase in the percentage of β-cells that had nuclear 53BP1 foci (from 2.77 ± 0.02 to 19.67 ± 1.2; $P < 0.01$) (Fig. 3*A*). Moreover, mice treated with STZ showed islet staining for phospho-Kap1 (Ser824), a histone modifier whose phosphorylation is a hallmark of ATM activity (30), which was similar to the pattern observed in the pancreas (both endocrine and exocrine) after γ-irradiation (Fig. 3*B*).

We next examined DDR in β-cells from NOD mice, a strain that spontaneously develops autoimmune diabetes (12). We documented 53BP1 patterns in NOD pancreas sections at 2, 7, and 10 weeks of age and immediately after the first blood glucose measurement >200 mg/dL (15–18 weeks of age). Age-matched outbred ICR mice were used as wild-type controls. Although NOD mice show insulitis from a very early age, we did not detect significant differences in the extent of 53BP1 activation between these mice and ICR controls at any age (Fig. 3*C*). Therefore, the NOD model does not recapitulate the increased DDR observed in β-cells from patients with T1D. The lack of evidence for β-cell DDR activation in NOD mice suggests that DDR is not obligatory for islet inflammation to occur and that islet inflammation by itself does not necessarily lead to activation of a β-cell DDR.

Finally, we studied the LEW.1AR1-iddm rat model of spontaneous T1D (13). In this model, a mutation in the gene encoding for Dock8 leads to an immune attack on islet cells, culminating in insulin-dependent diabetes mellitus (iddm) in 20% of the animals at ~60 days of age. We examined β-cell 53BP1 activation in tissue sections from prediabetic LEW.1AR1-iddm rats and healthy controls (Fig. 3*D*) and found, similarly to patients with T1D, that activated 53BP1 and γ-H2AX are more frequent in β-cells from iddm compared with nondiabetic controls (Fig. 3*D* and data not shown). Therefore, a β-cell DDR in vivo in the form of 53BP1 activation occurs in human T1D, in spontaneous rat T1D, and upon MLDS treatment of mice.

DNA Damage Induces Proinflammatory Gene Expression in Islets Ex Vivo and In Vivo

To explore the link between DDR and inflammatory signaling in islet cells, we exposed cultured murine islets to STZ (10). One hour after treatment, we isolated RNA from the islets and measured the expression of the proinflammatory molecules Ccl3, Ccl4, Ccl5, Ccl11, Cxcl10, IL-1β, IL-6, and TNF-α. Most of these cytokines have been reported to be elevated in islets of patients with recently diagnosed T1D (1,31). As a positive control, we applied recombinant TNF-α, a strong inducer of many of these cytokines (32). TNF-α and Cxcl10, a factor implicated in islet inflammation and T1D (31,33,34), were most strongly elevated upon STZ and TNF-α treatment (Fig. 4*A*). We also monitored the expression of cytokines in islets from MLDS mice immediately after the fifth injection and found increased levels of several proinflammatory cytokines, including Cxcl10 and IL-1β (Fig. 4*B*). These results show that DNA damage in mouse islets can evoke an immune response in the form of cytokine expression.

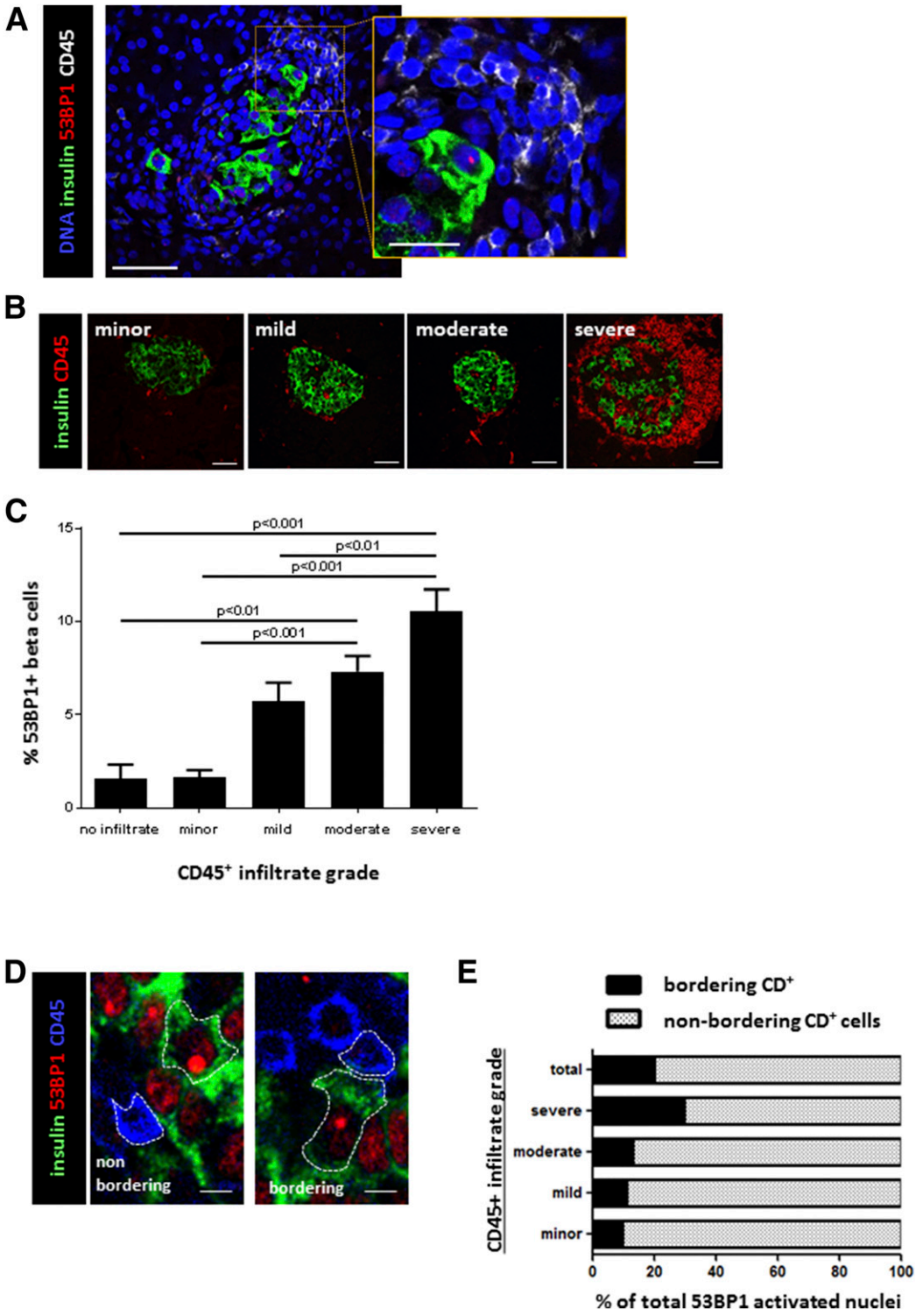

Figure 2—Association of human β-cell DNA damage with islet immune infiltration. *A*: Costaining for β-cell DNA damage and immune infiltration in a patient with recently diagnosed T1D. A β-cell (stained for insulin) with a 53BP1 nuclear focus is surrounded by a mass of small cells with compact nuclei that stained positive for the pan-leukocyte marker CD45 (inset). Scale bar = 10 μm, scale bar for inset = 3 μm. *B*: Classification of islets from patients with recently diagnosed T1D according to the extent of inflammatory infiltrate. Immunofluorescent staining for β-cells (insulin) and immune cells (CD45). The degree of infiltrate is determined by both the number of CD45 cells surrounding the islet and their level of islet penetrance. Scale bars = 10 μm. *C*: Scores of 53BP1 foci in islets from patients with recently diagnosed T1D according to the islet infiltration score. Shown are combined results from all recently diagnosed T1D samples that had insulin staining. *D*: High-magnification images demonstrating 53BP1-positive β-cells (insulin [green cytoplasm] and 53BP1 [red nuclear focus]) that are immediately adjacent to leukocytes (CD45) or are physically separated from such cells. Scale bars = 5 μm. *E*: Quantification of immunofluorescence images as those in *D*, showing the distribution of β-cells with activated 53BP1 according to proximity to $CD45^+$ cells (bordering and nonbordering).

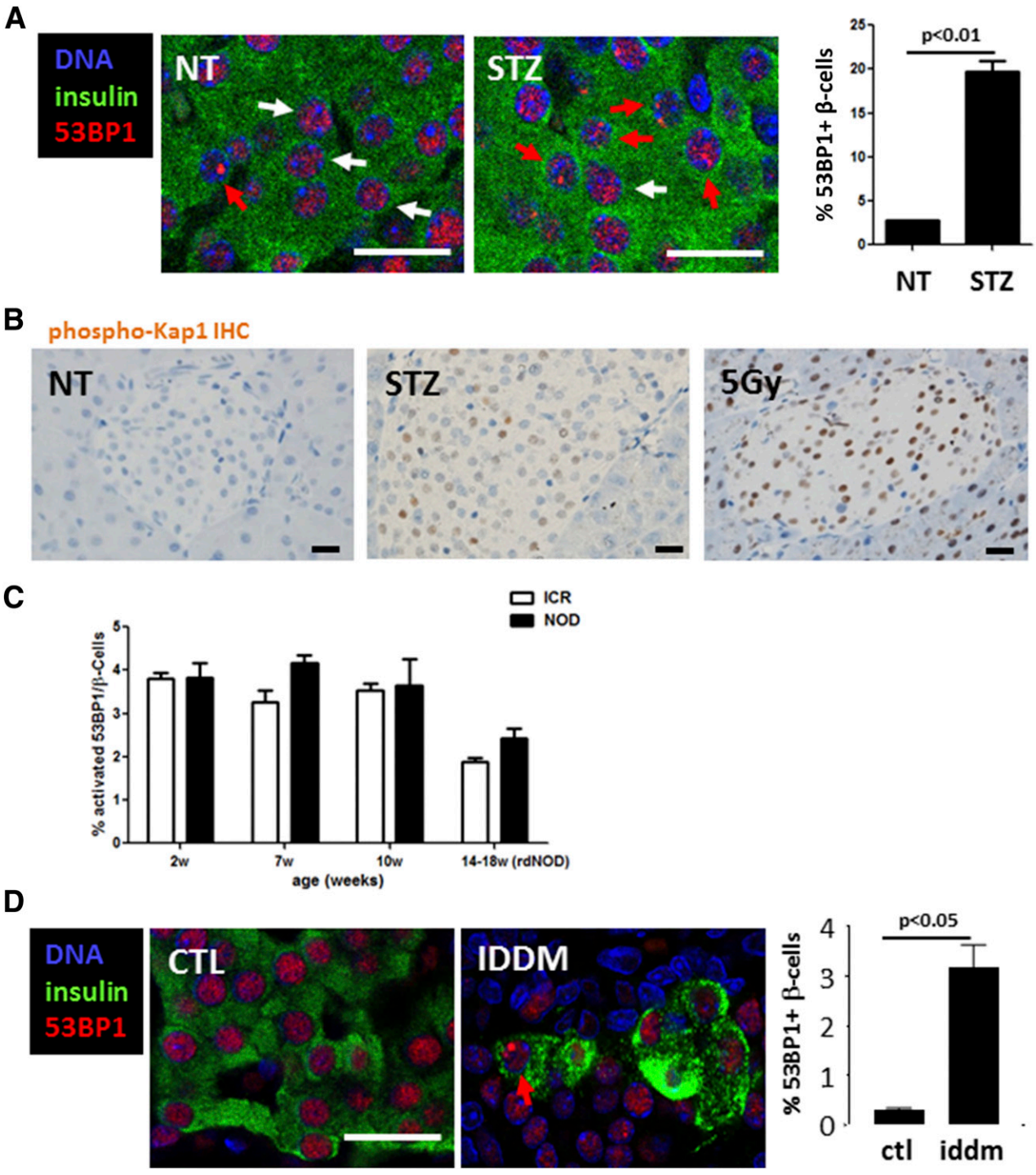

Figure 3—DDR in rodent models of diabetes. *A*: Immunostaining for 53BP1 in mouse β-cells in vivo after a single dose of 30 mg/kg STZ to wild-type mice. White and red arrows mark nuclei with nonactivated or activated 53BP1, respectively. Scale bars = 20 μm. Also shown is the quantification of the percentage of β-cell nuclei with nuclear 53BP1 foci. Untreated, n = 2 (NT); STZ (40 mg/kg) injected, n = 3. Error bars represent 1 SEM. *B*: Representative images from immunostaining for phospho-Kap1 in islets of control, single acute STZ-injected (200 mg/kg), and 5-Gy–irradiated mice. Nuclear accumulation of signal signifies Kap1 phosphorylation. Scale bars = 20 μm. *C*: Quantification of 53BP1 nuclear foci in islets of NOD and ICR control mice at various ages. *D*: Immunostaining for 53BP1 in healthy control (CTL) rats and in prediabetic LEW.1AR1-iddm rats and quantification of the 53BP1 nuclear foci in β-cells. Scale bar = 20 μm. IHC, immunohistochemistry; rdNOD, recently diagnosed nonobese diabetic mice; w, weeks.

ATM Mediates DNA Damage-Induced Cytokine Expression in Islets

A possible mediator of inflammatory cytokine transcription upon DNA damage is the double-strand break response factor ATM (30). We tested whether attenuation of ATM activation with the pharmacological inhibitor KU55933 (herein ATMi), could affect the response of islets to STZ ex vivo. We incubated wild-type murine islets with STZ

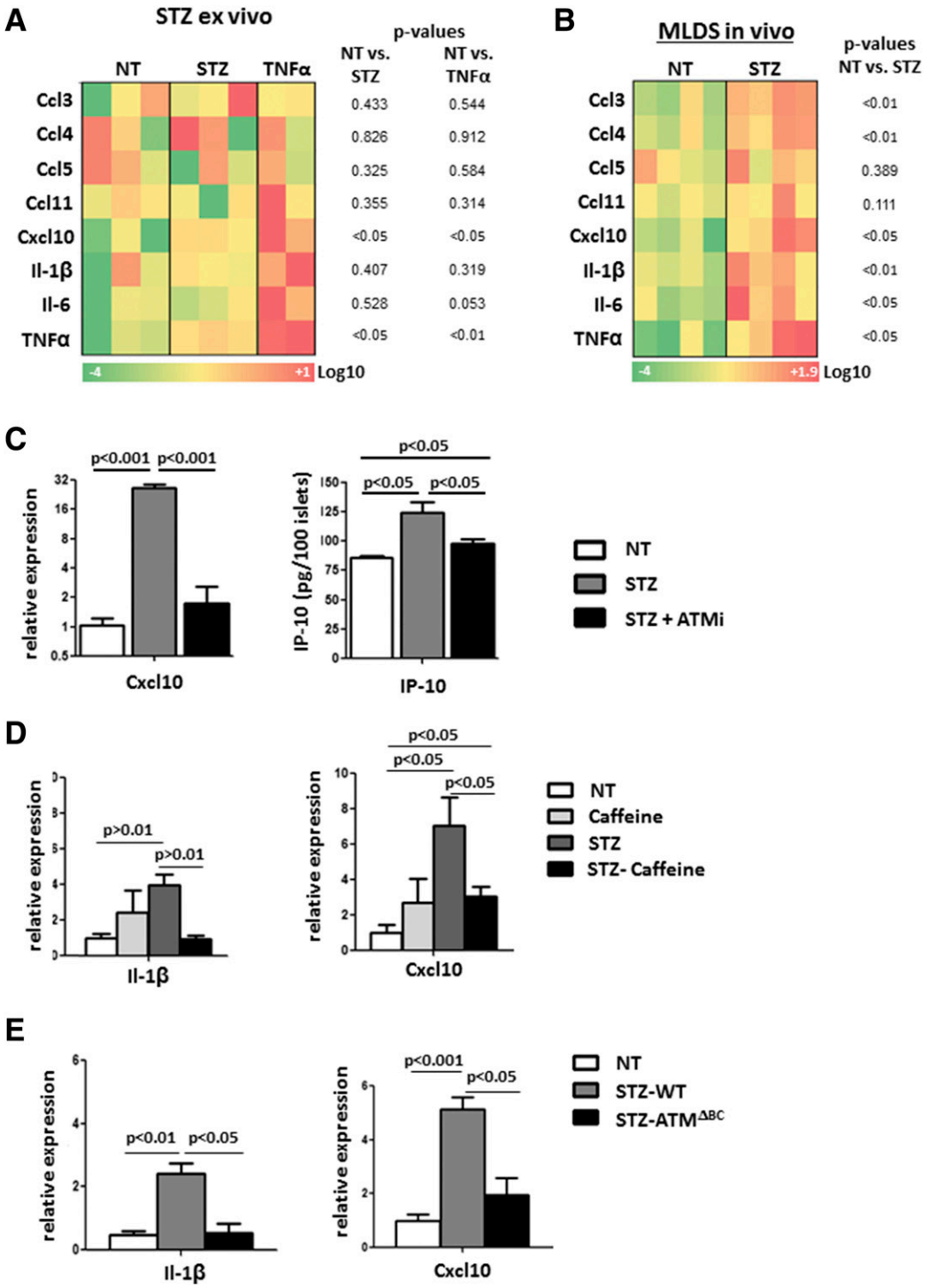

Figure 4—DDR through ATM induces proinflammatory cytokine expression in islets. *A*: Heat map presentation of qPCR of T1D-associated cytokines. Cultured mouse islets were treated with 5 mmol/L STZ or TNF-α for 1 h (pools of three different mice each). The *t* test *P* values are listed for each gene. *B*: Heat map presentation of qPCR of T1D-associated cytokines. Islets were harvested and analyzed after five daily STZ injections (20 mg/kg). The *t* test *P* values are listed for each gene. *C*: qPCR analysis of Cxcl10 performed on isolated wild-type mouse islets treated with 5 mmol/L STZ and 10 μmol/L KU55933 (ATMi) for 48 h. Error bars represent 1 SEM. Only statistically significant relations are connected. Also shown is an ELISA analysis of IP-10 performed on medium supernatants from the same experiment. Error bars represent 1 SEM. Only statistically significant relations are connected. *D*: qPCR analyses of IL-1β and Cxcl10 performed on islets from wild-type mice, untreated (NT) (saline injections) mice, and mice injected with caffeine (50 mg/kg), injected with STZ (20 mg/kg), and coinjected with STZ and caffeine (STZ-caffeine). All treatments were given for 5 consecutive days. Mice were sacrificed after the last injection. Error bars represent 1 SEM. Only statistically significant relations are connected. *E*: qPCR analyses of IL-1β and Cxcl10 performed on islets from NT wild-type mice (saline injections), wild-type mice injected with STZ (STZ-WT), and $ATM^{\Delta BC}$ mice injected with STZ (STZ-$ATM^{\Delta BC}$). STZ (20 mg/kg) was injected for 5 consecutive days. Mice were sacrificed after the last injection. Error bars represent 1 SEM. Only statistically significant relations are connected.

alone or with ATMi for 48 h and measured Cxcl10 expression and secretion. Cxcl10 was elevated upon exposure to STZ in both the mRNA (25.7 ± 2.43-fold; $P < 0.001$) and secreted protein levels (from 73.00 ± 2.50 to 124.6 ± 11.53 pg/100 islets; $P < 0.05$), and the response could be abrogated by coincubation with ATMi (1.68 ± 0.83-fold [$P < 0.001$] and 89.56 ± 5.02 pg/100 islets [$P < 0.05$]) (Fig. 4*C*).

To assess whether DDR plays a role in vivo in STZ-mediated proinflammatory gene expression, we applied the MLDS protocol together with general inhibition of the DDR through injections of the ATM/ATR general inhibitor caffeine (35). We found that mice coinjected with STZ and caffeine had a blunted induction of both Cxcl10 (3.04 ± 0.5-fold; $P < 0.05$ to untreated; $P < 0.05$ to STZ only) and IL-1β (0.98 ± 0.2 fold; $P < 0.01$ to STZ only) (Fig. 4*D*). These results suggest a link between DNA damage (induced by STZ) and an islet inflammatory response (Cxcl10 and IL-1β elevation) through a DDR factor (ATM).

To define more precisely the role of ATM in the response of islets to DNA damage, we generated mice with β-cell–specific deletion of the gene for *Atm* by crossbreeding mice with a conditional *Atm* allele (loxP-flanked exons 57–58 encoding the core phosphatidylinositol 3-kinase–related kinase kinase domain) (10) with Insulin-Cre mice (11). PCR analysis confirmed the deletion of the two ATM exons in the islets from compound Insulin-Cre; $ATM^{lox/lox}$ mice (herein termed $ATM^{\Delta BC}$) (Supplementary Fig. 3). mRNA levels of Atm in total islet lysates of the $ATM^{\Delta BC}$ were significantly lower than in littermate controls (an average decrease of ~50%; $P < 0.0001$) (Supplementary Fig. 3), with the remaining ATM likely derived from non–β-cells in the islets. To confirm effective inactivation of ATM in β-cells, we stained pancreatic sections of mice sacrificed at 1 h after γ-irradiation (5 Gy) for phospho-Kap1. As expected, irradiation led to a rapid accumulation of phospho-Kap1 in both the exocrine and the endocrine pancreas (Supplementary Fig. 3). In irradiated $ATM^{\Delta BC}$ mice phosho-Kap1 was missing specifically in islet cells, demonstrating the β-cell–specific ablation of ATM activity (Supplementary Fig. 3).

Untreated $ATM^{\Delta BC}$ mice displayed normal pancreas and islet morphology and a mild glucose intolerance upon challenge (data not shown) consistent with a previous report on impaired insulin secretion in mice globally deficient for ATM (36). We subjected mice to the MLDS model and evaluated the mRNA levels of Cxcl10 and IL-1β in islets of $ATM^{\Delta BC}$ and control mice. We observed an elevation of Cxcl10 (5.15 ± 0.4-fold; $P < 0.001$) and IL-1β (2.43 ± 0.3-fold; $P < 0.05$) in control MLDS islets, which was blunted in $ATM^{\Delta BC}$ mice (Cxcl10 1.94 ± 0.6 fold [$P < 0.05$], IL-1β 0.56 ± 0.2-fold [$P < 0.05$]) (Fig. 4*E*). These results provide genetic evidence that DDR signaling through ATM contributes to the development of insulitis under the MLDS model.

DDR Signaling Contributes to STZ-Induced Diabetes in Mice

We next asked whether reduced DDR in ATM mutants affects the development of diabetes induced by STZ. Of note, $ATM^{\Delta BC}$ mice exposed to MLDS demonstrated blunted development of hyperglycemia compared with control mice (Fig. 5*A* and *B*) (two-way ANOVA $P = 0.0058$). Moreover, a time course follow-up of mice with persistent hyperglycemia (>250 mg/dL) showed that $ATM^{\Delta BC}$ mice are largely resistant to MLDS diabetes-induced hyperglycemia (8 days median time to diabetes in controls, undefined median in $ATM^{\Delta BC}$ mice; log-rank $P = 0.0071$) (Fig. 5*C*). Mice carrying the Rip-Cre transgene alone (ATM proficient) responded to MLDS similarly to wild-type mice, ruling our nonspecific effects of the Cre transgene (Supplementary Fig. 3). It was also claimed that this driver transgene expresses hGH (37); however, we found that pancreatic tissue slides from Rip-Cre mice were negative for hGH staining (Supplementary Fig. 3).

To test whether the milder response to MLDS in ATM-deficient mice is related to an autoimmune process, we subjected $ATM^{\Delta BC}$ mice again to MLDS, this time sacrificing the cohort 5 days after the last injection. We immunostained pancreatic tissue from these mice for the T-cell marker CD3 (Fig. 5*D*). Quantification of the fraction of islets stained positive for CD3 revealed a marked difference between $ATM^{\Delta BC}$ mice and sibling controls. The area stained positive for CD3 in islets from the control group was 8.85 ± 1.2% compared with only 3.67 ± 0.2% in $ATM^{\Delta BC}$ mice (Fig. 5*E*). The reduced T-cell infiltration is consistent with decreased islet expression of the T-cell chemoattractant Cxcl10 in $ATM^{\Delta BC}$ mice (Fig. 4*E*) and supports the idea that DDR inhibition under the MLDS model can affect the extent of islet immune cell infiltration.

We then studied whether β-cell ATM deficiency prevents β-cell loss in MLDS. The insulin/glucose ratio, a measure of β-cell function, was reduced in wild-type MLDS mice but not in $ATM^{\Delta BC}$ MLDS mice compared with untreated controls (untreated mice 1 ± 0.13, wild-type STZ 0.32 ± 0.07, $ATM^{\Delta BC}$ STZ 0.95 ± 0.22; $P < 0.05$) (Fig. 5*F*). $ATM^{\Delta BC}$ STZ mice also displayed a higher proportion of area stained for insulin (1.18 ± 0.1%) compared with similarly treated wild-type sibling control mice (0.62 ± 0.1%; $P < 0.01$) (Fig. 5*G* and *H*) and a higher number of islets per section (wild-type STZ 9.6 ± 1.34, $ATM^{\Delta BC}$ STZ 15.2 ± 1.43; $P < 0.05$) (Fig. 5*I*). Thus, β-cell–specific ablation of ATM protects mice from experimental diabetes induced by MLDS.

Finally, we analyzed β-cell 53BP1 activation as a function of islet T-cell infiltration in $ATM^{\Delta BC}$ and control mice 5 days after the first STZ injection (Fig. 6*A*). Wild-type MLDS mice revealed an association between β-cell 53BP1 nuclear foci and the extent of islet T-cell infiltration (Fig. 6*B*), with noninfiltrated islets showing the lowest levels of 53BP1 activation and islets with a more extensive $CD3^+$ infiltrate having a higher index of 53BP1 activation. This result agrees with findings in samples from patients with recently diagnosed human T1D. Of note, the association between DDR and immune cell infiltration was abrogated by ATM deletion. $ATM^{\Delta BC}$ mice had higher levels of islet 53BP1 activation with all the various degrees of infiltration

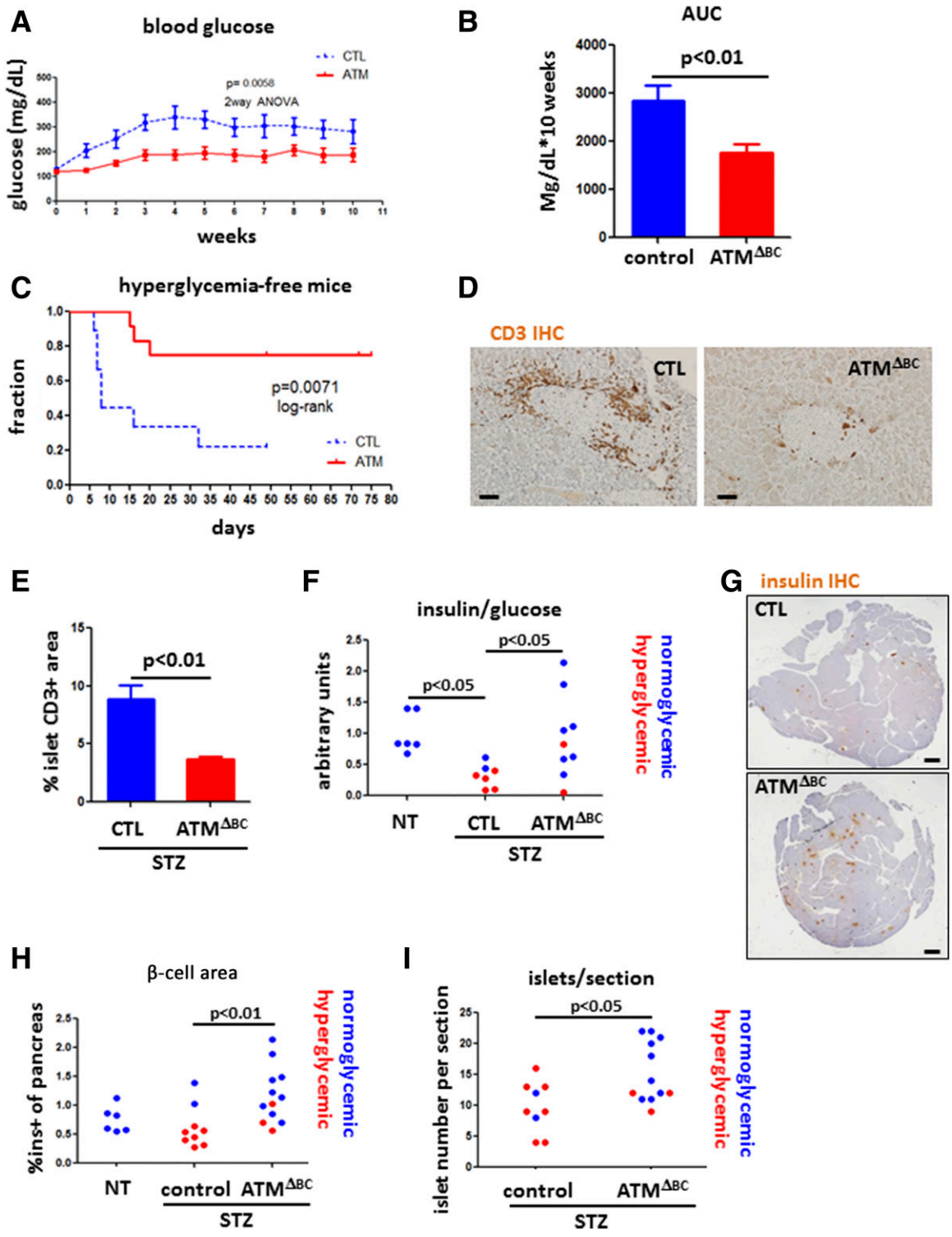

Figure 5— Attenuated development of STZ diabetes in mice with ATM-deficient β-cells. *A*: Average blood glucose levels of control (CTL) (n = 9) and ATM$^{\Delta BC}$ (n = 12) mice subjected to MLDS-STZ. Graph starts with the 1st day of five consecutive daily low-dose STZ injections. Shown are the combined results of three different iterations of the experiment. Error bars represent 1 SEM. *B*: Average area under the curve (AUC) of the glucose measurements in *A* (CTL, n = 9; ATM$^{\Delta BC}$, n = 12). *C*: Hyperglycemia-free survival curve of CTL (n = 9) and ATM$^{\Delta BC}$ (n = 12) mice subjected to MLDS. Hyperglycemic mice were defined by more than two consecutive measurements of glucose >250 mg/dL. *D*: Representative images from immunostaining for CD3. Scale bars = 20 μm. *E*: Quantification of the immunostaining in *D* (CTL, n = 2; ATM$^{\Delta BC}$, n = 3). Error bars represent 1 SEM. *F*: Insulin/glucose ratio in the blood of nontreated (NT) (CTL, n = 3; ATM$^{\Delta BC}$, n = 3), STZ-injected CTL (n = 7), and STZ-injected ATM$^{\Delta BC}$ (n = 9) mice. *G*: Insulin immunostaining in STZ-treated CTL and ATM$^{\Delta BC}$ mice. Scale bars = 1 mm. *H*: Quantification of the staining in *E*. *I*: Number of islets per section as determined by inspection of hematoxylin-eosin–stained sections of STZ-injected CTL (n = 9) and STZ-injected ATM$^{\Delta BC}$ (n = 12) mice. IHC, immunohistochemistry; ins+, insulin positive.

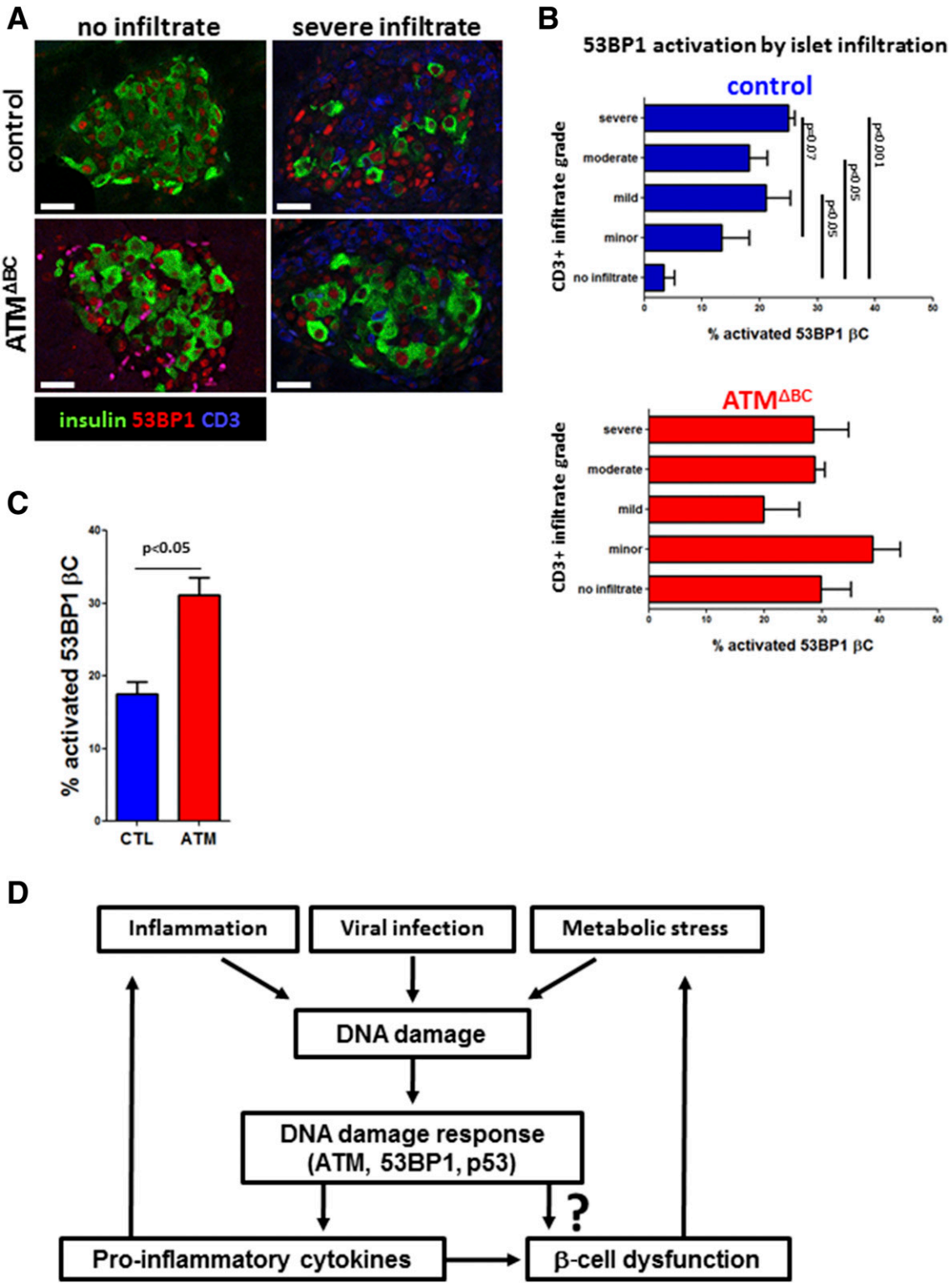

Figure 6—ATM ablation disrupts the DDR-insulitis association. *A*: Immunostaining for 53BP1 and CD3 in mouse β-cells in vivo. Mice received five daily injections of STZ (30 mg/kg) and were sacrificed 5 days after the last injection. Scale bars = 20 μm. *B*: Scoring for 53BP1 foci in islets from STZ-injected wild-type and ATM$^{\Delta BC}$ mice, according to the islet CD3 infiltration score. *C*: Overall percentage of β-cell 53BP1 nuclear foci in STZ-injected wild-type and ATM$^{\Delta BC}$ mice. *D*: Model of β-cell DNA damage caused by metabolic stress, inflammation, viral infection, or other injury that leads to a DDR that triggers a proinflammatory response. This may lead to islet dysfunction and exacerbation of islet inflammation. βC, β-cell; CTL, control.

(Fig. 6*B*), yet the overall presence of insulitis was lower. This finding suggests that an ATM-dependent β-cell DDR is important for T-cell recruitment. We also observed that the general activation of 53BP1 (all islets combined regardless of infiltration levels) was higher in the $ATM^{\Delta BC}$ group (Fig. 6*C*), which shows that in the MLDS model, DNA damage to β-cells can signal through ATM to recruit T-cells. We conclude that ATM-dependent DDR in β-cells promotes proinflammatory cytokine expression, islet T-cell infiltration, and diabetes.

DISCUSSION

We identified DDR as an early β-cell–specific injury in human T1D. Our analyses suggest that this phenomenon peaks around the clinical onset of the disease, a time in which islet inflammation is most prevalent. In addition to the temporal coincidence between DDR and islet inflammation, we found a physical association between insulitis and β-cell DDR. Our experiments in mice with genetic and pharmacological inhibition of ATM implicate DDR as a factor that may accelerate islet inflammation. Although islet inflammation is undoubtedly mediated by a complex molecular network, this study reveals the proinflammatory cytokines Cxcl10 and IL-1β as two potential mediators of DNA damage-induced islet inflammation. Of note, elevated Cxcl10 was reported in pancreas samples from a cohort of patients with newly diagnosed T1D (31). Cxcl10 is a potent chemoattractant for T cells (34,38), and indeed, that study reported an increase in the presence of immune cells expressing Cxcr3 (the Cxcl10 receptor) (31). These data suggest a pathway leading from β-cell DNA damage through ATM-dependent cytokine expression to islet inflammation and autoimmunity.

What is driving the β-cell DDR in T1D? The marked heterogeneity of DDR within β-cells of the same individual suggests that systemic hyperglycemia is unlikely a sole driver of the effect (14). The increased 53BP1 activation in islets of normoglycemic AAB+ donors confirms that it is not hyperglycemia that leads to this elevation. It is possible that β-cell heterogeneity (e.g., β-cells having different aging phenotypes or different sensitivities to metabolic stress) (39–41) results in a differential cellular response to systemic insults. It was previously shown that reactive nitrogen species can lead to DNA breaks in isolated islets (42) and that inducible nitric oxide synthase inhibition can prevent hyperglycemia after the MLDS protocol (43,44). Therefore, nitric oxide is a possible factor leading to β-cell DNA damage at early stages of T1D. Alternatively, it is possible that β-cell DDR is triggered by islet-infiltrating cells, although the lack of tight physical association between 53BP1-positive β-cells and immune cells argues against this possibility as an exclusive mechanism. Moreover, the increase in 53BP1-positive β-cells in AAB+ donors argues against induction of DDR by immune cells because insulitis was scarce in these samples. We hypothesize that both metabolic and inflammatory injuries may contribute to DNA damage in β-cells. In turn, the DDR may lead to further aggravation of β-cell dysfunction and immune attack, thus contributing to a vicious cycle ending with T1D (Fig. 6*D*). Another potential contributor to DDR in human T1D is viral infection. We have previously demonstrated a low-grade, persistent enterovirus infection in the same resection samples analyzed here (45), and others have shown that viral infection may trigger the DDR (25). Low-grade viral infection may give rise to cell stress and DNA damage, inducing both inflammation and β-cell death. Additional experiments are needed to examine the potential effect of viral infection on DDR in human T1D.

Although the effect of DNA damage is difficult to determine with the use of histological specimens of human T1D, our experiments with mouse islets ex vivo and with mice treated with STZ suggest a causal role for DDR in triggering islet inflammation and autoimmune diabetes. When ATM was absent in β-cells or inhibited pharmacologically, STZ-induced expression of proinflammatory cytokines, such as Cxcl10 and IL-1β, was blunted, as were islet infiltration and hyperglycemia, whereas islet cell mass and β-cell function were preserved. This suggests that the DDR in β-cells induces the expression and secretion of inflammatory cytokines, potentially contributing to autoimmune destruction of β-cells.

Our conclusions are consistent with several lines of evidence that have previously implicated β-cell DDR in T1D. First, the established diabetogenic β-cell toxin STZ is a DNA alkylating agent (28). Second, mice deficient for p53 (the activation of which during DNA damage depends on ATM) are resistant to STZ-induced autoimmunity (46), further supporting a chain of events that leads from DNA damage, through p53 and ATM, to immune system activation in support of the relevance of the MLDS-induced diabetes. Third, genetic polymorphisms in the DNA double-strand break repair genes XRCC4 and DNA ligase IV were reported to predispose to β-cell dysfunction in T1D (8).

We note the similarity between the cytokines observed in human T1D (1), in the LEW.1AR1-iddm rat model of human T1D (12,13), and the cytokines induced in a DDR-dependent manner in STZ-treated mice; both processes appear to share the involvement of nuclear factor-κB (NF-κB) and its targets, particularly the key proinflammatory cytokine IL-1β (47). Indeed, it was previously shown in the context of cancer that DNA damage can lead, through ATM, to the activation of NF-κB and its targets, including IL-1β (48). Moreover, NF-κB has been shown to control the induction of Cxcl10 after STZ administration, and β-cell NF-κB inhibition attenuated diabetes under MLDS (49). In conclusion, our findings suggest that DDR in β-cells may contribute to islet autoimmunity, β-cell death, and T1D.

Funding. The DiViD project was funded by the South-Eastern Norway Regional Health Authority (grant to K.D.-J.), by the Novo Nordisk Foundation (grant to K.D.-J.), and through the Persistent Virus Infection in Diabetes Network (PEVNET) Study Group funded by the European Union's Seventh Framework Programme

(FP7/2007–2013) under grant agreement 261441 PEVNET. This research also was performed with the support of nPOD, a collaborative T1D research project sponsored by JDRF International. Organ procurement organizations partnering with nPOD to provide research resources are listed at www.jdrfnpod.org/our-partners.php. Y.D. is supported by grants from JDRF, the Human Islet Research Network of the National Institutes of Health (DK-104216), The Leona M. and Harry B. Helmsley Charitable Trust, the European Union (project ELASTISLET), Britain Israel Research and Academic Exchange, the Israel Science Foundation, the DON Foundation, and by a pilot grant from The Leona M. and Harry B. Helmsley Charitable Trust George S. Eisenbarth nPOD Award for Team Science (to Y.D.). Work in the A.C.P. laboratory at Vanderbilt University was supported by grants from the National Institutes of Health (DK-89572, DK-104211, DK-108120, DK-106755, and DK-20593), JDRF, and Department of Veterans Affairs.

Duality of Interest. No potential conflicts of interest relevant to this article were reported.

Author Contributions. E.H., S.Z., A.S., M.F., T.L., T.D., N.H., N.W.-C., and A.K. performed experiments. E.H., A.S., A.K., B.G., and Y.D. wrote the manuscript. E.H., B.G., and Y.D. designed the study. L.K., A.C.P., M.B., and K.D.-J. contributed human material. A.J. and S.L. contributed rat material. E.H. and Y.D. are the guarantors of this work and, as such, had full access to all the data in the study and take responsibility for the integrity of the data and the accuracy of the data analysis.

References

1. Krogvold L, Wiberg A, Edwin B, et al. Insulitis and characterisation of infiltrating T cells in surgical pancreatic tail resections from patients at onset of type 1 diabetes. Diabetologia 2016;59:492–501
2. Herold KC, Usmani-Brown S, Ghazi T, et al.; Type 1 Diabetes TrialNet Study Group. β cell death and dysfunction during type 1 diabetes development in at-risk individuals. J Clin Invest 2015;125:1163–1173
3. Krogvold L, Skog O, Sundström G, et al. Function of isolated pancreatic islets from patients at onset of type 1 diabetes: insulin secretion can be restored after some days in a nondiabetogenic environment in vitro: results from the DiViD Study. Diabetes 2015;64:2506–2512
4. Tornovsky-Babeay S, Dadon D, Ziv O, et al. Type 2 diabetes and congenital hyperinsulinism cause DNA double-strand breaks and p53 activity in β cells. Cell Metab 2014;19:109–121
5. Tavana O, Zhu C. Too many breaks (brakes): pancreatic β-cell senescence leads to diabetes. Cell Cycle 2011;10:2471–2484
6. Tavana O, Puebla-Osorio N, Sang M, Zhu C. Absence of p53-dependent apoptosis combined with nonhomologous end-joining deficiency leads to a severe diabetic phenotype in mice. Diabetes 2010;59:135–142
7. Tavana O, Puebla-Osorio N, Kim J, Sang M, Jang S, Zhu C. Ku70 functions in addition to nonhomologous end joining in pancreatic β-cells: a connection to β-catenin regulation. Diabetes 2013;62:2429–2438
8. Dooley J, Tian L, Schonefeldt S, et al. Genetic predisposition for beta cell fragility underlies type 1 and type 2 diabetes. Nat Genet 2016;48:519–527
9. Wunderlich R, Ruehle PF, Deloch L, et al. Interconnection between DNA damage, senescence, inflammation, and cancer. Front Biosci 2017;22:348–369
10. Zha S, Sekiguchi J, Brush JW, Bassing CH, Alt FW. Complementary functions of ATM and H2AX in development and suppression of genomic instability. Proc Natl Acad Sci U S A 2008;105:9302–9306
11. Gannon M, Shiota C, Postic C, Wright CV, Magnuson M. Analysis of the Cre-mediated recombination driven by rat insulin promoter in embryonic and adult mouse pancreas. Genesis 2000;26:139–142
12. Lenzen S. Animal models of human type 1 diabetes for evaluating combination therapies and successful translation to the patient with type 1 diabetes. Diabetes Metab Res Rev 2017;33
13. Lenzen S, Tiedge M, Elsner M, et al. The LEW.1AR1/Ztm-iddm rat: a new model of spontaneous insulin-dependent diabetes mellitus. Diabetologia 2001;44:1189–1196
14. Porat S, Weinberg-Corem N, Tornovsky-Babaey S, et al. Control of pancreatic β cell regeneration by glucose metabolism. Cell Metab 2011;13:440–449
15. Pugliese A, Vendrame F, Reijonen H, Atkinson MA, Campbell-Thompson M, Burke GW. New insight on human type 1 diabetes biology: nPOD and nPOD-transplantation. Curr Diab Rep 2014;14:530
16. Krogvold L, Edwin B, Buanes T, et al. Pancreatic biopsy by minimal tail resection in live adult patients at the onset of type 1 diabetes: experiences from the DiViD study. Diabetologia 2014;57:841–843
17. Panier S, Boulton SJ. Double-strand break repair: 53BP1 comes into focus. Nat Rev Mol Cell Biol 2014;15:7–18
18. Noda A, Hirai Y, Hamasaki K, Mitani H, Nakamura N, Kodama Y. Unrepairable DNA double-strand breaks that are generated by ionising radiation determine the fate of normal human cells. J Cell Sci 2012;125:5280–5287
19. Hussain K, Padidela R, Kapoor RR, et al. Diabetes mellitus, exocrine pancreatic deficiency, hypertrichosis, hyperpigmentation, and chronic inflammation: confirmation of a syndrome. Pediatr Diabetes 2009;10:193–197
20. Rodriguez-Calvo T, Ekwall O, Amirian N, Zapardiel-Gonzalo J, von Herrath MG. Increased immune cell infiltration of the exocrine pancreas: a possible contribution to the pathogenesis of type 1 diabetes. Diabetes 2014;63:3880–3890
21. Pálmai-Pallag T, Bachrati CZ. Inflammation-induced DNA damage and damage-induced inflammation: a vicious cycle. Microbes Infect 2014;16:822–832
22. Salama R, Sadaie M, Hoare M, Narita M. Cellular senescence and its effector programs. Genes Dev 2014;28:99–114
23. Zhu P, Zhang D, Chowdhury D, et al. Granzyme A, which causes single-stranded DNA damage, targets the double-strand break repair protein Ku70. EMBO Rep 2006;7:431–437
24. Kawanishi S, Ohnishi S, Ma N, Hiraku Y, Oikawa S, Murata M. Nitrative and oxidative DNA damage in infection-related carcinogenesis in relation to cancer stem cells. Genes Environ 2017;38:26
25. Nakad R, Schumacher B. DNA damage response and immune defense: links and mechanisms. Front Genet 2016;7:147
26. Klammer H, Mladenov E, Li F, Iliakis G. Bystander effects as manifestation of intercellular communication of DNA damage and of the cellular oxidative status. Cancer Lett 2015;356:58–71
27. Pateras IS, Havaki S, Nikitopoulou X, et al. The DNA damage response and immune signaling alliance: is it good or bad? Nature decides when and where. Pharmacol Ther 2015;154:36–56
28. Lenzen S. The mechanisms of alloxan- and streptozotocin-induced diabetes. Diabetologia 2008;51:216–226
29. Goyal SN, Reddy NM, Patil KR, et al. Challenges and issues with streptozotocin-induced diabetes - a clinically relevant animal model to understand the diabetes pathogenesis and evaluate therapeutics. Chem Biol Interact 2016;244:49–63
30. Lavin MF, Kozlov S. ATM activation and DNA damage response. Cell Cycle 2007;6:931–942
31. Roep BO, Kleijwegt FS, van Halteren AG, et al. Islet inflammation and CXCL10 in recent-onset type 1 diabetes. Clin Exp Immunol 2010;159:338–343
32. Hayden MS, Ghosh S. Regulation of NF-kappaB by TNF family cytokines. Semin Immunol 2014;26:253–266
33. Antonelli A, Ferrari SM, Corrado A, Ferrannini E, Fallahi P. CXCR3, CXCL10 and type 1 diabetes. Cytokine Growth Factor Rev 2014;25:57–65
34. Corrado A, Ferrari SM, Ferri C, Ferrannini E, Antonelli A, Fallahi P. Type 1 diabetes and (C-X-C motif) ligand (CXCL) 10 chemokine. Clin Ter 2014;165:e181–e185
35. Sarkaria JN, Busby EC, Tibbetts RS, et al. Inhibition of ATM and ATR kinase activities by the radiosensitizing agent, caffeine. Cancer Res 1999;59:4375–4382
36. Miles PD, Treuner K, Latronica M, Olefsky JM, Barlow C. Impaired insulin secretion in a mouse model of ataxia telangiectasia. Am J Physiol Endocrinol Metab 2007;293:E70–E74
37. Brouwers B, de faudeur G, Osipovich AB, et al. Impaired islet function in commonly used transgenic mouse lines due to human growth hormone minigene expression. Cell Metab 2014;20:979–990
38. Christen U, von Herrath MG. IP-10 and type 1 diabetes: a question of time and location. Autoimmunity 2004;37:273–282

39. Johnston NR, Mitchell RK, Haythorne E, et al. Beta cell hubs dictate pancreatic islet responses to glucose. Cell Metab 2016;24:389–401
40. Weir GC, Bonner-Weir S. Glucose driven changes in beta cell identity are important for function and possibly autoimmune vulnerability during the progression of type 1 diabetes. Front Genet 2017;8:2
41. Aguayo-Mazzucato C, van Haaren M, Mruk M, et al. β cell aging markers have heterogeneous distribution and are induced by insulin resistance. Cell Metab 2017;25:898–910.e5
42. Kaneto H, Fujii J, Suzuki K, et al. Apoptotic cell death triggered by nitric oxide in pancreatic beta-cells. Diabetes 1995;44:733–738
43. Flodström M, Tyrberg B, Eizirik DL, Sandler S. Reduced sensitivity of inducible nitric oxide synthase-deficient mice to multiple low-dose streptozotocin-induced diabetes. Diabetes 1999;48:706–713
44. Mabley JG, Southan GJ, Salzman AL, Szabó C. The combined inducible nitric oxide synthase inhibitor and free radical scavenger guanidinoethyldisulfide prevents multiple low-dose streptozotocin-induced diabetes in vivo and interleukin-1beta-induced suppression of islet insulin secretion in vitro. Pancreas 2004;28:E39–44
45. Krogvold L, Edwin B, Buanes T, et al. Detection of a low-grade enteroviral infection in the islets of Langerhans of living patients newly diagnosed with type 1 diabetes. Diabetes 2015;64:1682–1687
46. Hoshino A, Ariyoshi M, Okawa Y, et al. Inhibition of p53 preserves Parkin-mediated mitophagy and pancreatic beta-cell function in diabetes. Proc Natl Acad Sci U S A 2014;111:3116–3121
47. Donath MY, Böni-Schnetzler M, Ellingsgaard H, Halban PA, Ehses JA. Cytokine production by islets in health and diabetes: cellular origin, regulation and function. Trends Endocrinol Metab 2010;21:261–267
48. Kanarek N, Grivennikov SI, Leshets M, et al. Critical role for IL-1β in DNA damage-induced mucositis. Proc Natl Acad Sci U S A 2014;111:E702–E711
49. Eldor R, Yeffet A, Baum K, et al. Conditional and specific NF-kappaB blockade protects pancreatic beta cells from diabetogenic agents. Proc Natl Acad Sci U S A 2006;103:5072–5077